

The Dynamic Effects of Weather Shocks on Agricultural Production ^{*}

Cédric Crofils¹ Ewen Gallic² Gauthier Vermandel³

February 24, 2023

Abstract

The paper investigates the dynamic effects of weather shocks on monthly agricultural production in Peru with local projections. An adverse weather shock, measured by an excess of heat or rain, always generates a negative downturn in agricultural production, but its magnitude and duration depend on several factors such as the type of crop concerned, the land geographical type and the season. On average, a weather shock can cause a monthly decline by 5% of agricultural production up to four consecutive months. The response is time and space dependent. A shock in tropical forest regions or occurring during growing season exhibits a much larger response. At a macroeconomic level, weather shocks entail a surge in inflation and reduction in aggregate production.

JEL classification: C23, E32, Q11, Q54

^{*}We thank Olivier Deschenes, Garance Genicot, Elise Huillery, Evi Pappa, Juan-Pablo Rud for their remarks, as well as seminar participants in University College London, Université Paris-Dauphine. Ewen Gallic acknowledges that the project leading to this publication has received funding from the French government under the “France 2030” investment plan managed by the French National Research Agency (reference :ANR-17-EURE-0020) and from Excellence Initiative of Aix-Marseille University – A*MIDEX. Gauthier Vermandel acknowledges funding from the chair Stress-test hosted by Institut Polytechnique de Paris. Cedric Crofils acknowledges funding from the Collectivité Territoriale de Martinique.

¹University Paris Dauphine – PSL Research University, LEDa UMR CNRS 8007, Place du Maréchal de Lattre de Tassigny, 75775 Paris Cedex 16, France. E-mail: cedric.crofils@dauphine.psl.eu.

²Aix Marseille Univ, CNRS, AMSE, Marseille, France. E-mail: ewen.gallic@gmail.com.

³Corresponding author. CMAP, Ecole polytechnique, Institut Polytechnique de Paris, Route de Saclay, 91128 Palaiseau Cedex. University Paris Dauphine – PSL Research University, LEDa UMR CNRS 8007, Place du Maréchal de Lattre de Tassigny, 75775 Paris Cedex 16, France. E-mail: gauthier@vermandel.fr

1 Introduction

Among all economic sectors, agriculture is the most vulnerable to fluctuations in the weather. In developing countries, the agricultural sector is a major contributor to aggregate production in terms of output and employment. In these economies, weather shocks can have wide economic consequences (Mendelsohn, 2009). Because many small-scale farmers in developing countries have limited access to risk management tools, such as insurance and irrigation infrastructure, these economies are also particularly vulnerable to exogenous shifts in weather conditions (Aragón et al., 2021). As a result, weather shocks can have a disproportionate impact on livelihoods and food security.

Given those vulnerabilities, the goal of this paper is to quantitatively measure the dynamic effects of abnormal weather realizations on the supply of agricultural products over time. Understanding and quantitatively assessing what consequences an unexpected weather event observed today has on future crop production is central to anticipate its adverse consequences. Such quantitative analysis can be used to make better informed decisions about planting or harvesting crop, to adapt to climate change at a farmer level. In addition, these quantitative assessments are critically important for policymakers to anticipate the potential food shortage and income loss, and thus to implement adequate mitigation policies.

The literature examining how the weather affects agricultural production typically bases its quantitative analysis on annual data (see, *e.g.*, Jagnani et al., 2020; D'Agostino and Schlenker, 2016; Burke and Emerick, 2016; Deschênes and Greenstone, 2007). However, the use of annual data probably underestimates the total cost of the weather as extreme positive and negative weather events average out throughout the year (Colacito et al., 2019). To be immune to these temporal aggregation effects, this study relies on monthly production data in order to examine the dynamic effects of the weather along the crop growth process. This process naturally creates a time lag between the shock realization and its materialization in terms of economic loss at harvesting time. This dynamic propagation mechanism shaped by the growing process of crops is to our knowledge yet unexplored in the literature (see Dell et al., 2014 for a literature review). The goal of this paper is therefore to evaluate the dynamic propagation over months of the weather, and analyze how land-specific factors such as geographical topology and stage of crop growth play a role in shaping the response of agricultural products to a random draw in the weather.

Our empirical approach investigates the impact of weather fluctuations on agricultural production in Peru, based on monthly regional and crop-specific data. The analysis em-

employs a linear panel model with local projections. The Peruvian agricultural sector in 2015 represented 7% of the country's GDP, 28% of employment, and used 18% of the total country's land. The Ministry of Agriculture and Irrigation of Peru provides agricultural data on a monthly basis at a region level between 2001 to 2015 for four types of crops: rice, maize, potato and cassava. The highly detailed region-crop-month data allows to precisely decompose how the weather affects agricultural production over months. Our measure of weather shocks is based on precipitation and temperatures: we extract the maximum regional extreme daytime weather data within a month, and express it into a weather anomaly by taking the distance of the variable from its historical average.¹ We study the effects of weather shocks on production rather than on yields. The literature traditionally studies yields rather than production. However, as indicated by [Iizumi and Ramankutty \(2015\)](#), when calculating agricultural yields, all information about the quantity produced and available is erased. In fact, in the event of a weather disruption to crop growth, farmers may choose to abandon a part of their production if the cost of harvesting outweighs the expected profit or if harvesting is no longer feasible. The yields observed at the end of the season will not reflect such decisions. This idea is echoed by [Lesk et al. \(2016\)](#), who additionally state that the volume of production plays a role in determining food security, whereas yields do not.

Local projections (LPs), pioneered by [Jordà \(2005\)](#), have become a widespread econometric tool to measure impulse response functions. LPs are relatively more robust to misspecification, easy to both estimate (via linear regression) and accommodate to panel data. We exploit the plausibly exogenous variation in temperature and precipitation at the Peruvian regional level to study the effects of weather shocks on agricultural production. We control for fixed regional attributes and macroeconomic characteristics. Then, by exploiting the cross-sectional dimension at the region-level, we use impulse response analysis to measure the propagation of a regional weather shock on agricultural production. The impulse response analysis is particularly well suited to dissect the cost of weather shocks that are disseminated over time through the natural growing process of crops.

Our paper is connected to two complementary literature branches. The first strand of literature examines the nexus between economic growth and climate based on yearly data. [Dell et al. \(2012\)](#) find on a large panel of countries that higher temperatures reduce economic

¹Intergovernmental Panel on Climate Change (IPCC) studies, such as [Parry et al. \(2007\)](#), have documented a large negative sensitivity of crop production to extreme daytime temperature and precipitation. We build on this observation to construct our weather variables.

growth as well as agricultural production. In the continuation of this paper, the research question has been next extended in many directions.² Colacito et al. (2019) provide a similar exercise for the US economy and find that rising summer temperatures have a pervasive effect in the entire cross-section of industries. Ortiz-Bobea et al. (2021) use panel regression at the country level and yearly data from 1961 to 2015 to investigate the impact of climate change on agricultural Total Factor Productivity (TFP). The authors find that on average, in Latin America, climate change has had a negative impact on agricultural TFP, reducing it by more than 25% over the sample period, as explained by the variations of average temperature and total rainfall.

The second strand of literature our paper is connected to estimates the effects of weather and climate change on agriculture. This literature can be divided into two branches: agronomic models based on crop simulations (see, *e.g.*, Rosenzweig et al., 2013; Asseng et al., 2014) and statistical models based on historical observations of agricultural production linked to weather observations. The economic literature has tended to rely more on statistical models. While early work used cross-sectional data (Mendelsohn et al., 1994), there has been a shift towards the use of panel data in the recent years. The dependent variable –crop yields, production, or profits– varies over both space and time. It is observed either directly at the farm level (see, *e.g.*, Welch et al., 2010; Powell and Reinhard, 2016; Schmitt et al., 2022) or at an aggregated geographical unit such as administrative regions (see, *e.g.*, Deschênes and Greenstone, 2007; Schlenker and Roberts, 2009; D'Agostino and Schlenker, 2016). The year-to-year variations of that variable are then modeled through a linear function of some weather variables. A group-specific effect –at the farm or administrative area level– that varies over time, and a time-specific effect that varies over groups are included to control for unobservable variables. The group-specific effect captures differences in factors such as soil quality between regions, which remain constant over time. On the other hand, the time-specific effect captures the impacts of variables such as exchange rate or inflation, which affect all regions similarly in a given year. By considering the year-to-year variations in the weather as exogenous, panel regressions can estimate the short-term effects of these unpredictable events on the dependent variable, capturing the dynamic response over time.³

²While most of the literature examines the effects of weather variables on quantities, Faccia et al. (2021) examine the effects on prices and finds desinflationary effects.

³As explained in Kolstad and Moore (2020), the use of panel regression and weather fluctuations to estimate the long-term effects of climate change is appropriate only if farmers cannot rapidly adapt to changing conditions. If farmers have the ability to rapidly adapt, then using this method to study the long-term responses of agriculture to climate change can lead to biased results, as it fails to account for the farmers' adaptation. To study long-term effects, Burke and Emerick (2016) suggest another framework

Furthermore, panel approaches are quite capable of predicting aggregate yields a few years ahead, as shown by [D'Agostino and Schlenker \(2016\)](#), at the US level. These authors estimate maize and soybean yields at the county level using annual historical data from 1950 to 2011. Once their models are estimated, they highlight that these panel models are able to convincingly predict yields over an out-of-sample period from 2012 to 2015, at the national level. For a more in-depth analysis of the strengths and weaknesses of panel data methods used to estimate the effects of weather or climate change on agriculture, see, *e.g.*, [Kolstad and Moore \(2020\)](#) and [Blanc and Schlenker \(2017\)](#).

The selection of weather variables to include in the analysis has received significant attention in the literature. Given that the dependent variable is typically observed annually, a temporal aggregation of weather data is necessary.⁴ [Ortiz-Bobea and Just \(2012\)](#) mention that most econometric models rely on weather variables aggregated over the growing season, with the underlying assumption that growing season dates are fixed in time. In this vein, some studies define accumulated metrics over the growing season, such as the growing degree days ([Schlenker and Roberts, 2009](#)). Other studies break down the growing season into several parts, based on the four seasons ([Schmitt et al., 2022](#)), or on weeks of the year ([Powell and Reinhard, 2016](#)). The division of the periods can also be done in order to match with different stages of the growing process, such as the vegetative phase, ripening, and maturation ([Ortiz-Bobea et al., 2019](#); [Welch et al., 2010](#)). The consideration of multiple points in time for aggregating weather variables stems from the idea that weather shocks can impact agriculture differently depending on when they occur. In fact, [Jagnani et al. \(2020\)](#), using survey data from Kenya revealed that farmers exhibit adaptation to weather shocks over the course of the growing season. Their findings indicate that in response to unexpected high temperatures, Kenyan farmers tend to increase pesticide use, decrease fertilizer application, and increase weeding efforts during the season. However, even when the weather data are aggregated across the different stages of production, the annual nature of the response variable prevents the study of the intra-season dynamics of the effects of weather shocks. Using monthly data and local projections, allows us to study these dynamic effects.

This paper brings three main contribution with respect to the literature. First, the high frequency of our data captures infra-annual variations in production and maps them with the corresponding weather fluctuations. While most of the literature uses annual panel data

in which they model the change in average yields at two different points in time for a given location as a function of changes in average temperature.

⁴The literature has also addressed the issue of spatial aggregation, which can lead to very different results depending on the method chosen. For more details, see [D'Agostino and Schlenker \(2016\)](#).

and exploits year-to-year variations by aggregating the weather conditions over the growing season, our approach allows for a finer estimation of the non-linear effects of the season. Using the context of Peru and its diversity in both geological and climatic conditions, we can distinguish geographical effects, leading to different responses according to the location of the weather shock.

Second, we employ the local projection method to examine the impact of weather fluctuations on production. Although this method has been used to estimate temperature shocks,⁵ its application on analyzing the agriculture-weather nexus is rather recent. LPs are particularly well-suited in this case to account for non-linear seasonal effects, which cannot be clearly determined with annual data.

Our last contribution concerns the role local weather shocks play in triggering aggregate fluctuations. Instead of focusing on the channel of impact directly on aggregate outcomes as literature usually does,⁶ we aggregate in-sample responses of regional crop production to weather shocks from LPs, in order to build a macroeconomic index of weather shock losses. We next include this new index into an otherwise standard vector auto-regressive model to quantitatively measure how weather shocks entail macroeconomic fluctuations.

Our main result is that an adverse weather shock always generates a negative downturn in agricultural production. The extent and duration of this decline depend on various factors such as the type of crops, the type of weather shock, the geographical pattern of agricultural land, and the season (growing season versus harvesting season). We find that a weather shock can cause a 5% monthly decline in agricultural production for up to four consecutive months for any crop type in the sample. Our second key finding highlights the role of geographical distribution of agricultural land in determining the response of agricultural production to weather shocks. We find that the response to weather shocks can be much greater in areas with tropical forests but much lower in coastal regions. Our third key finding emphasizes the role of crop growth timing in determining the response of agricultural production to weather fluctuations. A weather shock occurring during the growing season has a greater impact than one occurring during the harvest season.

The paper proceeds as follows. [Section 2](#) presents the data and the variables used in the empirical analysis. [Section 3](#) provides the estimation strategy and analyses the results of the panel estimation. [Section 4](#) investigates how the response of agricultural production to

⁵Natoli (2022) used this method to analyze the impacts of temperature surprises on the US economy on using quarterly data.

⁶See for example Acevedo et al. (2020) who find negative impacts of weather shocks on agricultural and aggregate output in developing countries.

a weather shock may differ accordingly with climate regions. [Section 5](#) explores the differentiated effects of weather shocks across production stages, distinguishing between a growth regime and a harvest regime. [Section 6](#) shifts the focus from agricultural production and examines the transmission of weather shocks to the rest of the national economy. [Section 7](#) concludes.

2 Data

This section provides a summary of the main data sources used for the empirical analysis.

2.1 Regional agricultural production data

Our main source of agricultural data comes from the monthly agricultural reports “*El Agro en Cifras*” produced by the Ministry of Agriculture and Irrigation of Peru (MINAGRI) from 2001 to 2019.⁷ Each report provides agroeconomic indexes and agricultural production at both a regional and national level. From these reports, we extract data on the production (in tons) and on the planted and harvested areas (in hectares) for each of the main crops cultivated in Peru at a regional level from January 2001 to December 2015. Note that observations after 2016 are no longer given on a monthly scale but only on a quarterly basis and are therefore excluded from our analysis. Each monthly report presents the data as cumulative sums between January and the month of the report. We apply a first difference filter to express production in net flows.

Four main crops are analyzed in this study: Potatoes (*papa*), Cassava (*yuca*), Rice (*arroz cáscara*), and Maize (*maíz amarillo duro*).⁸ The four crops selected in this study represent a significant share of agricultural production, both in terms of volume and surface: these crop varieties represent 53% of the cultivated surface and 37% of the total production in Peru.⁹ We compared our data to the Food and Agriculture Organisation data (FAOSTAT) to ensure their validity over the same years of observation and we find similar quantities (see [Table A.1](#) in the appendix). In the FAO data, our crop selection accounts for 41% of the

⁷Data are available for download at: <https://www.midagri.gob.pe/portal/boletin-estadistico-mensual-el-agro-en-cifras>.

⁸Two types of Maize are reported in the MINAGRI reports. In the rest of paper, we refer to “Dent corn” as “Maize.”

⁹The Peruvian agricultural report actually includes data for other types of crop, but the latter exhibits many missing observations and do not cover a sufficiently large time span in order to be included in the quantitative analysis.

cultivated surface and 31% of the total quantity produced. The small differences observed between the figures provided by the monthly reports produced by the Peruvian Ministry and those reported by the FAO are due to the fact that the former compile only the main crops while the latter are more exhaustive.

In agricultural economics, it is commonplace to express agricultural production into yields by dividing by the land surface planted. However, with monthly data, a significant number of observations exhibit zero value for the planted area, resulting in an inability to calculate yields for those months. In this paper, we propose to express agricultural production into percentage deviation from an average. The advantage of this procedure is twofold: first, it avoids arbitrarily excluding zero values for agricultural production, and second, it naturally corrects for the size effect stemming from regional heterogeneity in production. Our data transformation is addressed in two steps. For the subset of months $m \in t$ (e.g., all observations in January), we remove the trend by estimating the following OLS equation: $y_{cim}^{raw} = \alpha_0 + \alpha_1 t + \alpha_2 t^2 + \varepsilon_{cim}$, where c denotes the crop type and i the region, and ε_{cim} is a Normally distributed error term with zero mean. Let y^d denote the detrended expression, we finally deseasonalize by dividing each month by its monthly average as follows:

$$y_{c,i,t} = \ln(y_{c,i,t}^{det}) - \ln(\bar{y}_{c,i,m}^{det}), \quad (1)$$

where $\bar{y}_{c,i,m}^{det}$ denotes the monthly average of detrended production of crop c in region i at specific month m .

2.2 Regional weather data

As previously mentioned, agricultural production is subject to weather fluctuations. From daily grid temperature and precipitation data, we construct weather shock series, aggregated at the monthly level, for each of the 24 regions of Peru. In a nutshell, we follow [Barrios et al. \(2010\)](#) and demean the weather observation at the grid level. The means are the monthly historical values observed in the previous 20 years. Then, we aggregate the values at the region level and at a monthly scale. The obtained variables –the temperature and precipitation anomalies– are simply deviations from the average. The rest of this subsection provides the main steps to express raw weather data into regional weather anomalies.

Grid temperature data. We obtained data from PISCOt V1.1, a gridded daily temperatures data set available for Peru. The data runs from Jan 1981 to Dec 2016. The grid

has a 0.1° spatial resolution (10 km). The data set is developed by the SENAMHI (the National Service of Meteorology and Hydrology of Peru). The methodology that led to the construction of this data set is explained in [Huerta et al. \(2018\)](#).¹⁰

Grid precipitation data. The rainfall data are obtained from the CHIRPS v2.0 database, made available by the Climate Hazards Center of the UC Santa Barbara. Covering the quasi totality of the globe, the data set provides daily information on rainfall on a 0.05° resolution satellite imagery, from 1981 to present. The complete presentation of the data can be found on the Climate Hazards Center’s website ([Funk et al., 2015](#)) and the data set is freely available online.¹¹

From grid to regional data. Agricultural production is available at the regional level. It is therefore necessary to map grids and regions to aggregate the weather data at the regional level. In addition, shocks such as excessive temperatures or rainfall occurring in an agricultural area should not be accounted for in the same way as shocks occurring on urban geographic land. For example, the weather conditions of a grid cell where 90% of the surface is used for agricultural production should matter more than a cell with 10% of agricultural surface. When aggregating the weather data we need to identify beforehand where the agricultural regions are located in Peru, to give those regions more weight in the aggregation procedure. To do so, we rely on the data from Copernicus, a European program for monitoring the Earth using satellite and ground data, managed by the European Commission.¹² We use the 2015 Peru’s data, with a 100m resolution.

Regional weather anomalies. What is a relevant weather shock to predict agricultural production? [Parry et al. \(2007\)](#) have documented a large negative sensitivity of crop production to extreme daytime weather variables. We build on this observation to construct our two weather variables by taking the most daily extreme weather value within a month. To do so, let $\mathcal{W}_{i,y,m,d}$ denote one of the two weather measures –temperature or precipitation– observed in region i at day $d = \{D1, D2, \dots, D31\}$, month $m = \{M1, M2, \dots, M12\}$ and year $y = \{2001, 2002, \dots, 2015\}$.¹³ A weather shock is defined here as the most extreme meteorological

¹⁰Data can be obtained from <https://drive.google.com/drive/folders/1eGqhmJXBjFfSzUFz2RVqtbKIIOphpkcs>.

¹¹See <https://data.chc.ucsb.edu/products/CHIRPS-2.0/>.

¹²The data are freely available: <https://land.copernicus.eu/global/products/lc>. The share of agricultural land for each grid cell is shown on a map in [Figure 2](#) in the Online Appendix.

¹³Note that the weather data are given on a grid, on a daily basis. For more clarity in the notations, we write the equations on a regional and monthly scale. However, following [D’Agostino and Schlenker \(2016\)](#), the transformations of the weather data were first performed at the scale of the cells of the grid and then

logical event observed over the sequence of days within the considered month m in region i :

$$\mathcal{W}_{i,y,m} = \max(\{\mathcal{W}_{i,y,m,d}\}_{d=1}^{31}).$$

Note that taking the maximum, instead of some monthly average, avoids that extreme positive and negative events average out throughout the period (Colacito et al., 2019).

To assess the relative intensity of one weather shock with respect to other realizations, we measure the distance of the weather variable from its monthly average:

$$W_{i,t} = \mathcal{W}_{i,y,m} - \bar{\mathcal{W}}_{i,y,m},$$

where $\bar{\mathcal{W}}_{i,y,m} := (y_T - y_0)^{-1} \sum_{y=y_0}^{y_T} \mathcal{W}_{i,y,m}$ denotes the average value of the weather data during the specific month m observed over y years (between y_0 to y_T). Note that this procedure takes away the seasonal component of the weather. Therefore, $W_{i,t}$ denotes the deviations of the weather variable with respect its average, and is interpreted as a weather anomaly.

Going back to temperatures data, we apply the weather anomaly formula. Temperature anomaly $T_{i,t}$ is given by:

$$T_{i,t} = \mathcal{T}_{i,y,m} - \bar{\mathcal{T}}_{i,y,m}, \quad (2)$$

where $\mathcal{T}_{i,y,m}$ is the maximum of the monthly maximal temperature observed in month m of year y , y being within our time interval of interest (*i.e.*, 2001–2015), and where $\bar{\mathcal{T}}_{i,y,m}$ is the corresponding average for month type m over all the years available data (*i.e.*, $y_0=1881$ and $y_T=2016$). We interpret a large value of $T_{i,t}$ as an excess of heat (in °C) with respect to its historical average.

A similar indicator for the precipitation anomalies is computed, using the monthly sum of daily precipitation. It is compared to its monthly historical average:

$$P_{i,t} = \mathcal{P}_{i,y,m} - \bar{\mathcal{P}}_{i,y,m}, \quad (3)$$

where $\mathcal{P}_{i,y,m}$ is the sum of daily precipitation in month m of year y and where $\bar{\mathcal{P}}_{i,y,m}$ is its historical average. We interpret a large value of $P_{i,t}$ as an overabundance of humidity (in millimeters of rain) with respect to its historical average.

aggregated at a monthly frequency for each region. In other words, the temperature anomalies were first computed for each cell of the grid, and were aggregated after.

2.3 Macroeconomic data

Our sample also includes macroeconomic data that are used in our econometric approach as control variables. These control variables are useful to purge the variable of interest from unrelated sources of fluctuations with respect to the weather, and therefore isolate the effect of a weather variable on agricultural production. By holding constant the values of control variables, any changes in the outcome can be attributed solely to the variable of interest, rather than the combined effects of multiple variables. This makes it possible to draw more accurate conclusions about the causal relationship between the weather shocks and the agricultural output. To consider these potential effects, control variables based on macroeconomic data for the Peruvian economy are included. Namely, the monthly Peruvian CPI, the monthly Sol/US Exchange rate, the monthly national interest rate and the monthly GDP index.¹⁴ Note that all the control variables are national aggregates given on a monthly basis. Nominal variables (e.g. exchange rate and CPI) are detrended by calculating the growth rate. A similar transformation is applied on the interest rate, as the latter exhibits a downward trend on the time span considered. Finally, the GDP is expressed in percentage deviation from the Hodrick-Prescott filter, in order to control our projections from effects stemming from aggregate demand and supply shocks.

2.4 Summary statistics

This section introduces the main interesting features concerning the data. [Table 1](#) presents some descriptive statistics about the monthly production of the selected crops, averaged over the regions. One can observe an important variation in the production, which is also highly crop-specific. We remove from our data the negative values for production, which are due to different revaluations of production data estimates. We also exclude the regions where no tons were produced during our sample period. Columns 7 and 8 report respectively the number of producing regions and the number of observations for each type of crop.

In addition to this table, [Figure 1](#) provides a visual representation of the national production of each time of crop over our time sample, which is the sum of the monthly regional production. Interestingly, some cultures exhibit a clear and regular pattern (for Potato and Rice) while others are more volatile. We observe also that Cassava seems to present a pos-

¹⁴All macroeconomic data are taken from the data warehouse of *Banco Central de Reserva del Peru* (BCRP).

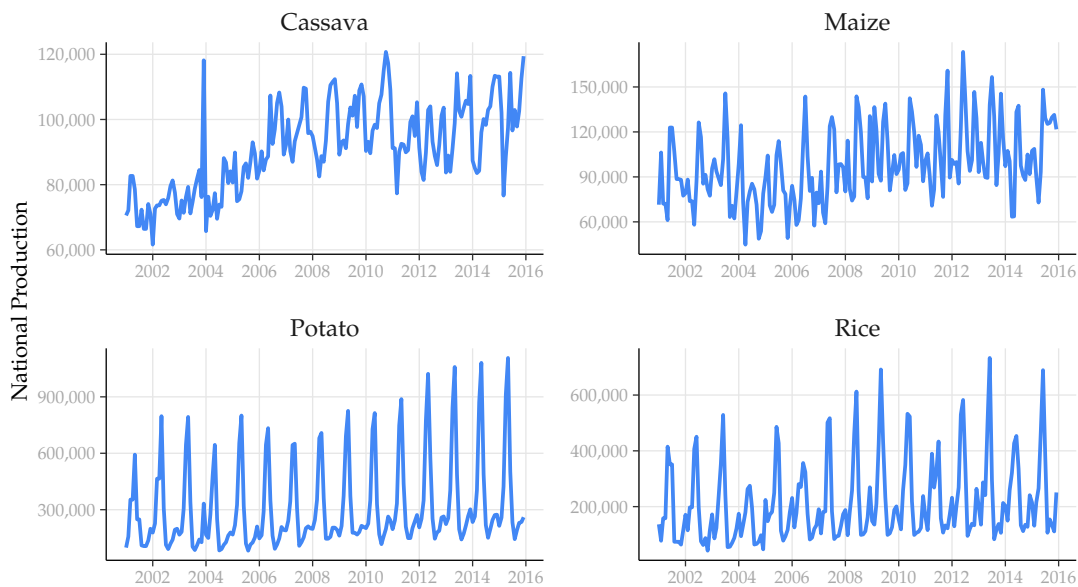
itive trend.¹⁵ We consider these features in the following sections by deseasonalizing the data.

Culture	Mean	Median	Standard Deviation	Min.	Max.	Nb. of regions	Nb. of obs.
Cassava	6,004.5	3,878.0	7,792.5	0.0	16,079.9	15	2,631
Maize	7,169.7	4,336.0	8,490.5	0.0	2,704.6	13	2,271
Potato	17,252.1	5,801.0	30,155.5	6.0	360,070.0	12	2,091
Rice	13,127.7	4,441.3	16,212.9	3.9	8,863.4	7	1,212

Notes: Quantities are reported in tons.

Source: MINAGRI. Author's estimate

Table 1: Descriptive statistics for monthly production (in tons) per type of crop



Notes: The graphs show the evolution of monthly crop production, summed over all administrative regions. For cassava, two observations (2007-06-01 and 2007-07-01) were incorrect and were replaced by a linear interpolation between May and July 2007.

Source: MINAGRI. Author's estimate

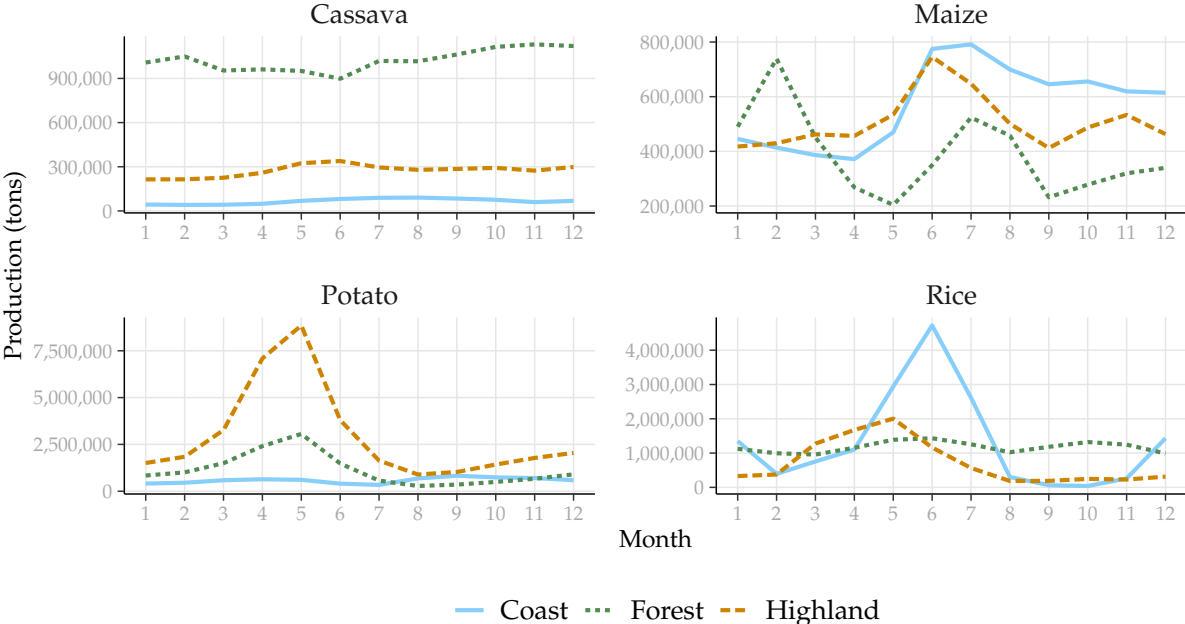
Figure 1: National monthly crop production for selected cultures (in tons)

Peru is geographically very diverse in terms of climate and geographical topology and is usually divided in three types of climate areas: Coast, Highlands and Amazon Rain-forest.

¹⁵This positive trend is possibly due to the increase in agrarian land, resulting from the deforestation of the Amazon rainforest, where a large share of cassava is produced. See [Figure 3](#).

These areas exhibit very different climatic conditions due to their proximity to the sea and their different altitudes. As explained in [Aragón et al. \(2021\)](#), the Coast area is a narrow strip extending from the seashore up to 500 meters above sea level (masl). It is situated in a semi-arid climate, with warm temperatures and little precipitation. The highlands extend from 500 up to almost 7,000 masl, albeit most agriculture stops below 4,000 masl. They have a much cooler and wetter climate, with seasonal precipitation in spring and early summer. Finally, the Amazon Rainforest area is continental and is characterized by a tropical weather with important rainfalls. A map dividing the Peruvian territory into these three natural regions is provided in [Figure A.2](#) in the Appendix, based on data available on the Geo GPS Peru website.¹⁶

The natural regions do not necessarily coincide with the administrative regions. Consequently, for each region, three variables are constructed, respectively indicating the share of each type of natural region in the administrative region.

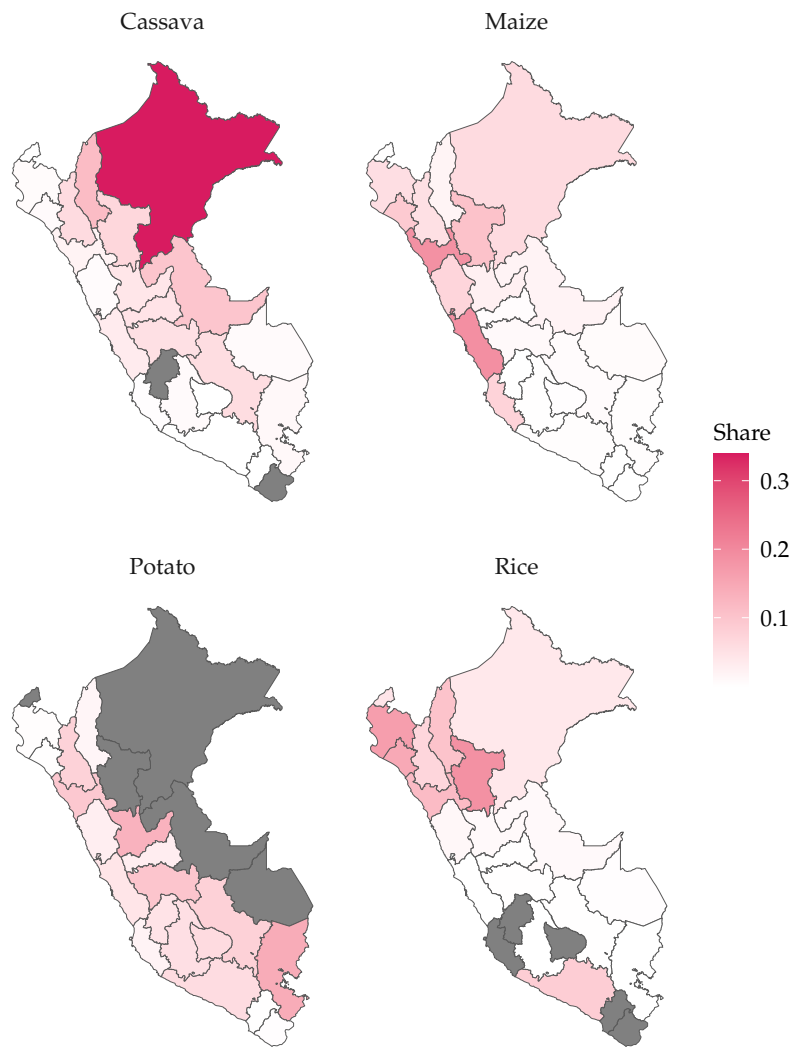


Notes: The graphs show the sum of each crop production, broken down by month and weighted by share of natural region.
Source: MINAGRI. Author's estimate

Figure 2: Crop production by months and natural regions (in tons)

¹⁶See <https://www.geogpsperu.com/2019/11/mapa-de-regiones-naturales-costa-sierra.html>.

In [Figure 2](#), we document the regional differences and the seasonality by averaging the monthly production over the different types of natural regions. In these graphics, the seasonal patterns can be observed more closely. For example, Potato production is sharply increasing between March and May, before decreasing after. Even if we account for the seasonality in the data by deseasonalizing them, the effects of weather might differ depending on the season. We investigate further this effect in [Section 5](#). In contrast, Maize displays differentiated seasonal cycles, depending on the natural regions. In coastal regions, we notice that there is only one production peak, in June. In forest areas, there are two main peaks, the higher in February and a smaller one in July. Those differences in season, associated with different climates depending on the natural region, call for a geographical analysis that we perform in [Section 4](#). Finally, the example of Cassava shows that the production can be highly concentrated in one area, here in the Forest where more than half of the production is located. On the other hand, Maize production is more evenly distributed. [Figure 3](#) below presents in more detail the production distribution for each type of crop.



Notes: Distribution of the production of each crop by administrative regions. For each map, the sum of of the distribution across regions equals 1. Non-producing regions are shown in gray.

Source: MINAGRI. Author's estimate

Figure 3: Regional distribution of crop production by administrative regions

3 The Dynamic Effects of Weather Shocks

How do weather shocks dynamically affect agricultural production? This section provides a discussion of the econometric approach, and then discusses the main results obtained from an impulse response function analysis.

3.1 Empirical Approach

Our empirical framework follows a similar conceptual framework from Dell et al. (2012). To fix ideas, consider the following simple economy characterized by a Cobb-Douglas technology in the agricultural sector in region i for crop c :

$$Y_{c,i,t} = A_{c,i}N_{c,i,t}H_{c,i,t}, \tag{4}$$

where the agricultural output for crop type c planted in region i at time t is denoted Y , crop-regional total factor productivity A , labor demand N and harvesting H . Note that in this expression, $A_{c,i}$, captures how regional conditions –such as local labor productivity– shape the productivity of labor for crops planted in this region. In contrast, $N_{c,i,t}$ embeds the macroeconomic fluctuations stemming from the labor market (*e.g.*, all aggregate shocks realized in t determining the country-wide real wage). Lastly, $H_{c,i,t}$ represents the surface harvested with N units of labor.

How does the weather interfere in the production process of agricultural goods? Consider that each period, farmers in region i plant a crop c on a land surface L . A typical process of crop growth cycle implies a lag between planting and harvesting times, referred to as the *growing season*. During the growing season, crops are vulnerable to weather shocks such as droughts and floods, leading to reduced growth and yields. In addition to these direct effects, weather shocks also lead to increased stress on the plants, making them more vulnerable to diseases. In severe cases, a drought can cause complete crop failure.

To capture these delayed effects of the weather on agricultural yields, let T_c denote the monthly duration of the crop-specific growing season between planting time ($h = 0$) and harvesting time ($h = T_c$). Therefore, it is assumed that $L_{c,i,t}$ units of planted land yields $L_{c,i,t} \exp\left(\sum_{h=0}^{T_c} \beta_{c,h}W_{i,t-h}\right)$ effective units of productive land, where the weather shock $W_{i,t-h}$ realized in $t - h$ affects crop production in harvested t with elasticity $\beta_{c,h}$.¹⁷ Weather shocks

¹⁷Note that we do not include a squared value for the weather variable. Squared terms are typically introduced to capture low frequency effects of climate change. In this paper, the time frequency is monthly.

are considered from the farmer’s perspective as exogenous variables that affect land productivity along the growing season. Weather variables, stacked in W , are formally connected to agricultural output as follows:

$$H_{c,i,t} \leq L_{c,i,t} \exp \left(\sum_{h=0}^{T_c} \beta_{c,h} W_{i,t-h} \right). \quad (5)$$

In this expression, it is assumed that the land surface planted $L_{i,c,t}$ exhibits both seasonal and trend components stemming from soil quality across time and space. Assuming that all planted surface is harvested, Equation 5 binds to equality. Note, however, that in presence of severe weather shocks, if the marginal cost of harvesting exceeds the marginal profits of land, it might be optimal for the farmer to partially harvest the planted surface.

Combining Equation 4 and Equation 5, and applying logs yields the following expression:

$$\ln \left(\frac{Y_{c,i,t}}{L_{c,i,t}} \right) = \ln (A_{c,i}) + \sum_{h=0}^{T_c} \beta_{c,h} W_{i,t-h} + \ln (N_{c,i,t}). \quad (6)$$

The left-hand-side of this equation represents the percentage deviation of agricultural production from its potential value, measured by $L_{c,i,t}$.

A natural question at this stage is to gauge how important is the elasticity of agricultural production to a change in weather conditions, namely inferring the value of $\beta_{c,h}$. We use local projections (LPs) based on Jordà (2005) to estimate how weather shocks impact agricultural output along the growing season of crops. In this paper, our two main exogenous variables are precipitation and temperature anomalies described in the data section. The interest of LPs is to allow for dynamic responses while neither imposing the estimation of the whole auto-regressive model nor introducing exogeneity restrictions. To estimate these effects, we run a local projection for $h = \{0, 1, \dots, T_c\}$ of the form:

$$y_{c,i,t+h} = \alpha_{c,i,h} + \beta_{c,h}^T T_{i,t} + \beta_{c,h}^P P_{i,t} + \delta_{c,i,h} X_t + \varepsilon_{c,i,t+h}, \quad (7)$$

where h denotes the time horizon considered. Consistently with Equation 6, agricultural production $y_{c,i,t+h}$ is deseasonalized and expressed in percentage deviation from a trend.¹⁸ Parameter $\alpha_{c,i,h}$ is the regional fixed effect that captures the time-invariant factors, such as

The use of a squared term is unlikely to change the sign nor the significance of our results.

¹⁸Recall that an OLS regression is employed with a seasonal fixed effects as well as a quadratic trend to infer the potential production of crops measured by $L_{c,i,t}$ in Equation 6.

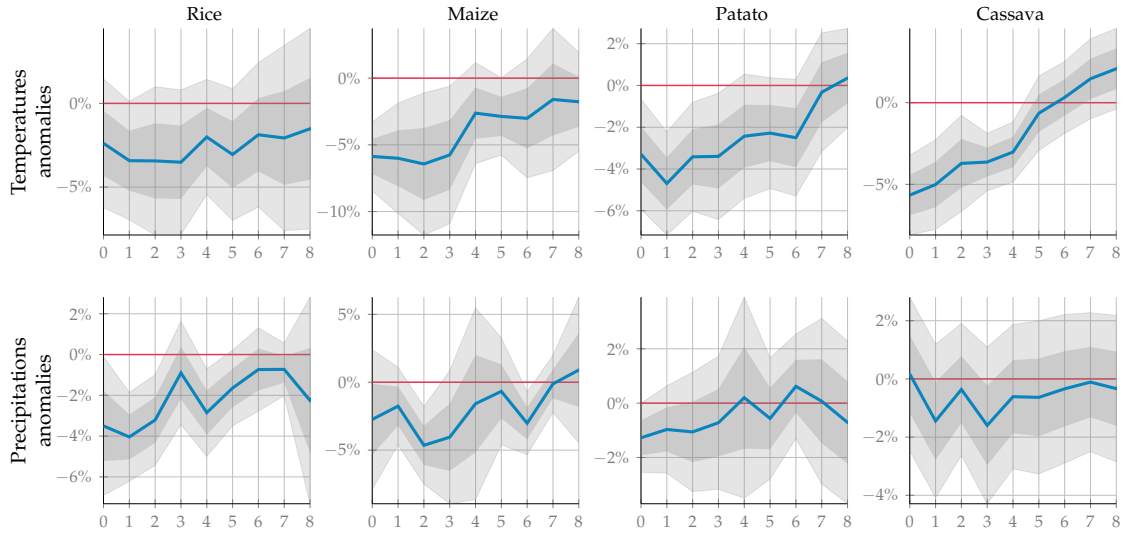
the local productivity level of labor or soil quality in region i . Note also that terms $T_{i,t}$ and $P_{i,t}$ represent the two distinctive weather variables that are considered in the inference exercise, namely the temperature and precipitation anomaly variables (described in [Subsection 2.2](#)). The two sequences of coefficients associated to the weather variables, $\beta_{c,h}^T$ and $\beta_{c,h}^P$, are of first order interest as they provide how much sensitive agricultural output is to exogenous changes in the weather variables. In addition, X_t is the set of control variables that capture contributions from aggregate fluctuations, as stacked in the labor demand term in [Equation 6](#). Control variables include the growth rate of the Exchange Rate (RER) growth rate, the seasonally adjusted industrial production expressed as a percentage deviation from the trend calculated by HP filter, the inflation rate and the growth of the interest rate. The set of coefficients $\delta_{c,i,h}$ are unknown and need to be estimated in the inference exercise. Finally $\varepsilon_{c,i,t+h}$ is an error term that is assumed to be white noise with zero mean.

3.2 Impulse response functions results

Estimated coefficients given in [Equation 7](#) are multiplied by a standard deviation of the weather variable to obtain the impulse response of the agricultural production to a standard weather shock. The responses are reported in [Figure 4](#) for a nine period horizon, contrasting for four different crops considered. A response to a one standard-deviation shock of temperature anomalies is reported on top, and for precipitation anomalies at the bottom.¹⁹ In both cases, a positive shock is considered: a one standard deviation increase in temperature and a one standard deviation increase in precipitation, both with respect to their historical averages. Positive deviations of temperature or precipitation anomalies correspond to higher than usual values.

The first row of [Figure 4](#) shows the response of agricultural production following a positive temperature shock. Overall, the shock leads to a sharp decrease in production for several months. However, the effects of this shock is often crop-specific due to the heterogeneous characteristics of the four type of crops considered. For example, temperature shocks on maize, potato and cassava lead to an abnormally lower than usual production, especially if the temperature shock occurs close to the harvesting time (*i.e.*, when the local projection horizon is close to zero). The percentage of production lost is about 5% per month for about 5 to 6 months. In contrast, rice exhibits a smaller albeit more persistent decrease in

¹⁹Note that the number of regions is not the same across crops as some regions do not produce specific types of agricultural products. We refer to [Table 1](#) for the description of agricultural production per regions and crop types.



Notes: The panels show the crop-specific impulse response function of monthly agricultural production to a one standard deviation (SD) increase in the weather variable, *i.e.*, a 1 SD increase with respect to the historical average. The weather variable is temperature anomaly for the first row and precipitation anomaly for the second row. Horizon 0 is the month of the shock. Shaded areas represent the 95% and 68% confidence intervals with region-level clustered standard errors.

Source: Author's estimates.

Figure 4: Agricultural production response to a weather shock

production, suggesting that this crop type is more temperature-tolerant.

The second row of panels in [Figure 4](#) reports the response of agricultural production following the realization of a precipitation anomaly shock in $h = 0$. A positive realization of the shock is associated with wetter than usual weather, more specifically, a one standard deviation increase in total precipitation relative to the historical average. With respect to temperature anomaly shocks, a precipitation anomaly exhibits a similar pattern, but with a response of a relatively smaller magnitude. Excess rainfalls are detrimental to agricultural production leading to a average agricultural production between 2 and 5%. As explained in [Skees et al. \(2007\)](#), El Niño events in Peru devastated a number of regions with massive flooding that washed away crops.²⁰ The presence of tropical climate, characterized by already abundant rainfalls, induces a large decrease in agricultural production following the realization of the precipitation anomaly shock. Although the shocks display a similar pattern, each crop reacts differently to the shocks through the timing and the magnitude of their response.

Variations in production following a precipitation shock are also highly crop-specific, and

²⁰[Crost et al. \(2018\)](#) find that an increase in wet-season rainfall is harmful to crops and produces more conflict in Philippines.

more volatile than responses to temperature shocks. Rice and maize are clearly affected during the first months consecutive to the shock, and then the effect becomes more variable and less significant. The two tuber crops, *i.e.*, cassava and potato, although sensitive to temperature shocks, show small and insignificant responses to abnormally high precipitation. Specific conditions due to the topology of the region may be a factor in explaining this apparent low sensitivity of production to precipitation variations. [Section 4](#) investigates this effect, by differentiating cultures according to their geographical environment.

4 The geographical dimension of weather shocks

The previous section highlighted that the response of agricultural production to a weather shock is crop-specific. In addition to the crop dimension, the spatial one can also be an important determinant of the vulnerability of agricultural production to the weather. Peru, as discussed in [Subsection 2.4](#), is indeed subject to different climatic conditions from one region to another. In particular, the climates that the country faces are different according to its natural regions, namely the coasts, the highlands and the Amazon rainforest. This section intends to address the geographical specificity of agricultural production responses to weather shocks.

4.1 Conceptual framework

To assess how much the geographical patterns quantitatively shape the role of weather shocks on agricultural production, consider the toy model presented in the previous section. It was previously assumed that land was homogeneous across regions. Consider now that each region, $L_{c,i}(\omega)$, exhibits idiosyncratic climatic characteristics ω , such that geographical patterns affect crops differently across regions as follows: $L_{c,i}(\omega) \exp\left(\sum_{h=0}^{T_c} \beta_{c,h,\omega} W_{i,t-h}\right)$. As discussed previously, Peru's geographical patterns can be stacked into three categories, such that ω is discrete and can take three values $\omega = \{\mathcal{C}, \mathcal{H}, \mathcal{F}\}$, *i.e.*, coast, highlands, and forest, respectively. Each type of geographic pattern can be associated with a production technology that is combined in a Cobb-Douglas manner:

$$H_{c,i,t} \leq \prod_{r \in \{\mathcal{C}, \mathcal{H}, \mathcal{F}\}} \left[L_{c,i,t}(r) \exp\left(\sum_{h=0}^{T_c} \beta_{c,h,r} W_{i,t-h}\right) \right]^{\gamma_{i,r}}. \quad (8)$$

where $\gamma_{i,r}$ denotes the intensity of the r^{th} type of geographical land in the total surface planted in region i .

Plugging [Equation 8](#) into the production function, and applying logs yield the following expression:

$$\ln \left(\frac{Y_{c,i,t}}{L_{c,i,t}} \right) = \ln (A_{c,i}) + \sum_{r \in \{\mathcal{C}, \mathcal{H}, \mathcal{F}\}} \gamma_{i,r} \sum_{h=0}^{T_c} \beta_{c,h,r} W_{i,t-h} + \ln (N_{i,c,t}). \quad (9)$$

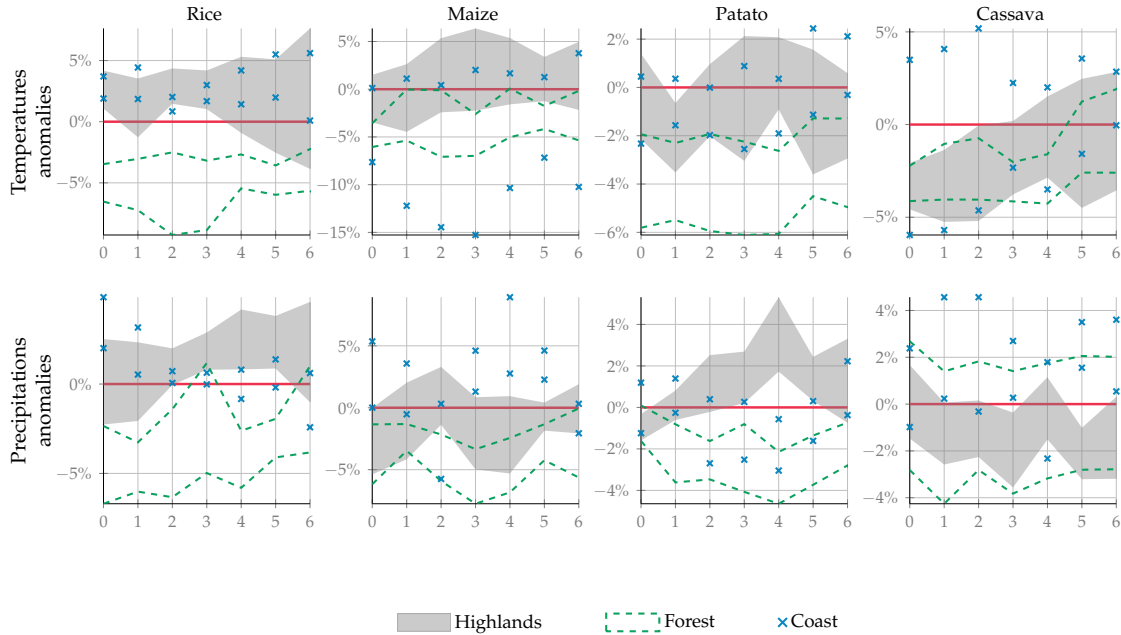
where potential production is a geometric average of different types geographical land, $L_{c,i,t} = \prod_r L_{c,i,t}(r)^{\gamma_{i,r}}$. The assumption of constant return to scale in land is maintained through the restriction: $\gamma_{i,\mathcal{C}} + \gamma_{i,\mathcal{H}} + \gamma_{i,\mathcal{F}} = 1$.

Our new LPs framework that takes into account regional patterns consistently with the theoretical setup in [Equation 9](#) is given by:

$$y_{c,i,t+h} = \alpha_{i,h} + \sum_{r \in \{\mathcal{C}, \mathcal{H}, \mathcal{F}\}} \gamma_{i,r} (\beta_{c,h,r}^T T_{i,t} + \beta_{c,h,r}^P P_{i,t}) + \delta_{i,h} X_t + \varepsilon_{c,i,t+h}, \quad (10)$$

where $\gamma_{i,r}$ is here an observable value that is computed based on the grid data covering Peru from the Geo GPS Peru website mentioned in [Section 2](#).

[Figure 5](#) reports the local projection obtained by estimating [Equation 10](#). The graphs in the first row of the figure present the response of abnormally hot temperature shocks for each selected crop while those in the second row concern abnormal precipitation shocks. Again, as in [Section 3](#), one standard deviation shocks are reported. Responses are differentiated by type of climate regions. Overall, the response to weather shocks is strongly altered when considering the geographical topology of land, in particular for coastal and forest regions. Responses for forest are furthermore predominantly more statistically different from zero.



Notes: The panels show the crop and geographical specific impulse responses of monthly agricultural production to a 1 SD increase in the weather variable. The weather variable is temperature anomaly for the first row and precipitation anomaly for the second row. Horizon 0 is the month of the shock. The bands formed by the grey area, the green dashed lines and the blue crosses represent the 95% confidence intervals with standard errors clustered at the region-level, for the Highlands, the Forest and the Coast regions, respectively.

Figure 5: Agricultural production response to a weather shock by taking into account geographical patterns (Highlands, Forest and Coast)

Let us start with the precipitation shocks. The responses for regions in forest areas exhibit a stronger negative effect of abnormally heavy rainfalls. This result is in line with our observations in Section 3. While the effects in the highlands and the coast remain positive albeit low, they are strongly negative and significant in forested areas. Also, by not distinguishing between types of climatic regions, the positive precipitation shocks are globally negative although not significantly different from zero. More importantly, this suggests that increases in precipitation are detrimental for already wet regions, while it may improve production to a lesser extent in dryer regions. We notice that the negative effect of abnormally abundant precipitation is driven by the forestry regions only for rice, maize and potatoes.

This last result also confirms that responses to shocks remain highly crop-specific. For example, rice produced in highland areas or in coastal regions can be better off with warmer than usual temperatures while such weather changes are always detrimental for rice produced in forested areas. In contrast, higher temperatures are always detrimental –or non significant– for cassava production, at least in the short run. Interestingly, for some crops

cultivated equally in coastal regions and in the mountains, responses to shocks are similar, while for other crops, the responses are quite different. For example, production of rice is evenly distributed between the coast and the highland in the north of Peru. In these regions, production is affected in the same manner by a precipitation shock. However, for potato production, also distributed almost evenly across the coast and the highland, the responses are quite different, with a positive response in the highlands and a negative one in the coast.

5 Time-varying exposure to weather shocks

A large body of the literature has found that the effects of weather shocks in agriculture critically depend on crop growth stages. For example, [Welch et al. \(2010\)](#) show differential effects of increases in minimum and maximum temperatures on rice yields in tropical/subtropical Asia depending on the growth phase. [Letta et al. \(2022\)](#) find that weather shocks triggers food prices rise during the growing period. [Masseti et al. \(2016\)](#) examine empirically how weather shocks within a growing season affect maize and soybean harvests using US county-level data. Crops need different types of nutrients depending on the stage of development of the plant. Excessively high temperatures or water volumes can be very detrimental to crop growth at some stages of growth while having little or no effect at other stages.

This section aims to capture this effect by exploiting the high frequency of our data. Indeed we can track the amount of crop that is planted and harvested each month. Rather than usual growing versus harvesting season dummy in annual data analysis, our measure of the growing season is a monthly continuous variables weighting the flow of land planted versus harvested. Although it is not possible to identify each development stage with the data at hand, we can distinguish the growing period (*i.e.*, when the planted surface is increasing) from the harvesting period (*i.e.*, when the harvested surface is increasing). The response of agricultural production to weather shocks can then be studied under two different regimes. To do so using local projections, we adapt the framework developed by [Auerbach and Gorodnichenko \(2011\)](#) for fiscal policy, and accommodate it to allow for state-dependent effects of the weather with a smooth transition between two distinctive stages: the growing and harvesting stages.

5.1 A state-dependent framework

Recall the toy model of agricultural production from [Equation 5](#). In this section, we will modify this model to endogenize the decision of planting crops.

Let $p_{c,i,t}$ denote the new surface planted and $h_{c,i,t}$ its harvested counterpart at time t for crop type c in region i . The net flow of new planted surface is therefore given by $p_{c,i,t} - h_{c,i,t}$. The total fraction of land with growing crops is measured here as the cumulative sums of flows in cultivated land surface over lifetime of a crop T_c as follows: $z_{c,i,t} = \sum_{h=0}^{T_c} (p_{c,i,t-h} - h_{c,i,t-h})$. To compare regions on a regular basis, we remove the possible trend and divide by the standard error as follows, $\hat{z}_{c,i,t} = (z_{c,i,t} - z_{c,i,t}^{HP}) / \sigma_{c,i,t}$, where $\hat{z}_{c,i,t}$ is our and zero-mean standardized index variable of utilized land surface. To express this index into a transition function with support $[0,1]$, it is assumed that our planted surface variable follows a logistic distribution $\hat{z}_{c,i,t} \sim L(\gamma_c)$ where $F(\hat{z}_{c,i,t})$ is the cumulative density function:²¹

$$F(\hat{z}_{c,i,t}) = \frac{1}{1 + \exp(-\gamma_c \hat{z}_{c,i,t})} \quad (11)$$

Letting $F(\hat{z}_{c,i,t})L_{c,i,t}$ denote the fraction of the potential land that is planted, $F(\hat{z}_{c,i,t})$ is both interpreted as a mass of land planted, or a degree of exposure of agricultural production to weather changes. Parameter γ_c captures the smoothness of the transition function, the transition becoming steeper as γ_c increases. Note that this parameter is crop-specific, as it captures how quick each type of crop is switching from its growing to harvesting stage. We discuss its numerical determination later on.

Consider now that weather effects depend of the growing stage of crops. The harvesting season is interpreted as the period when the mass of land planted $F(z_{c,i,t})$ is low (close to zero). In contrast, the growing season corresponds to the situation in which $F(z_{c,i,t})$ is high (close to one). Contrasting for the effects of the weather on the growing and the harvesting season, the surface of harvested land can be written as follows:

$$H_{c,i,t} \leq L_{c,i,t} \exp \left(\sum_{h=0}^{T_c} (F(\hat{z}_{c,i,t-h})\beta_{c,G}^h + (1 - F(\hat{z}_{c,i,t-h}))\beta_{c,H}^h) W_{i,t-h} \right), \quad (12)$$

where $\beta_{c,G}^h$ and $\beta_{c,H}^h$ are the response of agricultural production during the growing season, and during the harvesting season, respectively.

²¹Note that following [Auerbach and Gorodnichenko \(2011\)](#), this type of transition function is common in the context of LPs.

Injecting this term into the production yields to the following expression:

$$\ln \left(\frac{Y_{c,i,t}}{L_{c,i,t}} \right) = \ln (A_{c,i}) + \sum_{h=0}^{T_c} (F(\hat{z}_{c,i,t})\beta_{c,G}^h + (1 - F(\hat{z}_{c,i,t}))\beta_{c,H}^h) W_{i,t-h} + \ln (N_{i,c,t}). \quad (13)$$

The LPs framework can be accommodated again to analyze the role of growing versus harvesting season in the propagation of shocks. We examine the non-linear influence of the season in the response of each crop production to weather shocks. The same local projection method is used, but augmented with a state-dependent variable to allow for non-linear responses as in [Auerbach and Gorodnichenko \(2011\)](#). The framework takes into account the probability to be in growing season or in harvesting season:

$$\begin{aligned} y_{i,c,t+h} = & F(\hat{z}_{i,c,t}) [\alpha_{G,i}^h + \beta_{G,T}^h T_{i,c,t} + \beta_{G,P}^h P_{i,c,t} + \delta_{G,i}^h X_t] \\ & + (1 - F(\hat{z}_{i,c,t})) [\alpha_{H,i}^h + \beta_{H,T}^h T_{i,c,t} + \beta_{H,P}^h P_{i,c,t} + \delta_{H,i}^h X_t] + \varepsilon_{i,c,t+h}, \end{aligned} \quad (14)$$

where $y_{i,c,t+h}$ is still the deseasonalized production, and $T_{i,c,t}$, $P_{i,c,t}$, and X_t are, respectively the temperature and precipitation anomalies and the control variables, as defined in [Equation 7](#). The difference with this latter equation is that we now estimate the associated coefficients conditionally on the state of the season. Note that $\beta_{H,T}^h$ and $\beta_{H,P}^h$ are therefore the parameters of interest for the harvesting season, while $\beta_{G,T}^h$ and $\beta_{G,P}^h$ are the ones for the growing season. Following [Auerbach and Gorodnichenko \(2011\)](#), we also allow for seasonal-dependent fixed effects and marginal effects for control variables.

A key question at this stage is to determine γ_c , the parameter shaping the transition speed. [Auerbach and Gorodnichenko \(2011\)](#) typically calibrates this parameter to 1.5 without extensively discussing this choice. In contrast, we propose to empirically ground the value of γ_c by selecting the value maximizing log-likelihood function averaged over the 8 period horizon of the LPs. We obtain a crop-specific parameter that best fits the observed variations in agricultural productions for each type of product. We limit the support of γ_c to the range $[1, 10]$. A low value would make the transition probability to flatten to 0.5, while a high value would increase the transition speed without drastically changing the LPs, but would lead to small marginal gain in terms of log-likelihood.

The transition parameter exhibits heterogeneity across crops. The best value of γ_c for each type of crop is reported in [Figure 6](#). Rice and maize exhibit a relatively high value for γ , suggesting that transition from harvesting to growing season is relatively faster. In contrast, Potato and Cassava exhibit a relatively lower transition speed.

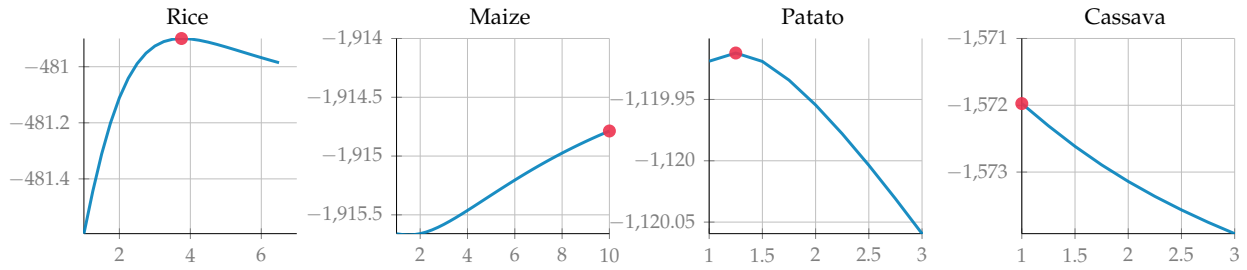


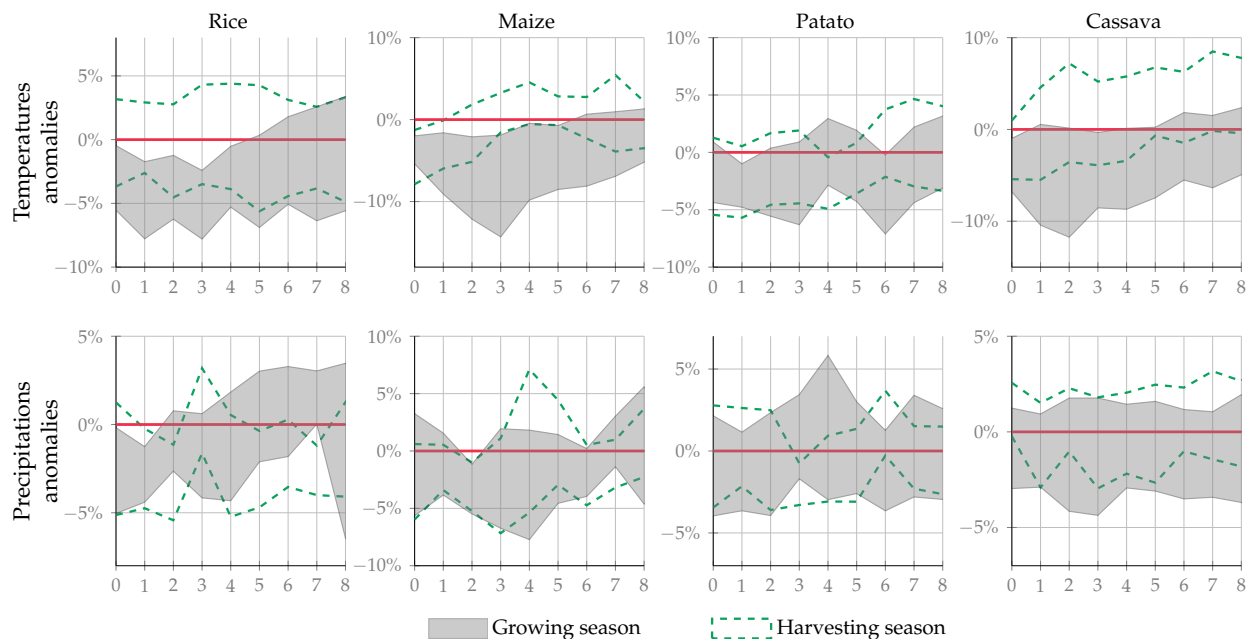
Figure 6: Average log-likelihood function for various values for transition speed parameter γ_c

5.2 Season-dependent impulse response functions

Figure 7 reports the response obtained from Equation 14. As before, the first row presents the crop-specific responses to a one standard deviation temperature anomaly shock, while the second row is the responses to a precipitation anomaly shock. Responses are distinguished by regime: the grey area represents the responses during the growing season while areas between the green dashed lines refer to the harvesting one. Confidence intervals are reported at a 95% confidence level.

The distinction between growing and harvesting season play an important role. Overall, we observe a differentiated impact with smaller –and quasi-null– effects when the shock happens during the harvesting season. In contrast, if the shock occurs during the growing season, the responses are in all cases negative and tend to have long-lasting effects on the production. This important result is in line with earlier studies such as Hatfield and Prueger (2015). These authors find that when a temperature shock happens during the growing stage of the crop development, it may affect the crop growth, which in turn leads to fewer yields. However, if the shock occurs when the crop is about to be harvested, then only a shock of high magnitude (severe drought, hail, landslide...) is likely to affect production significantly. Strikingly, the effect is common to all cultures, which underscores the importance of taking into account the different effects of the seasons.

Yet, as in the previous sections, we observe crop-specific responses, with differences in magnitude and duration of the detrimental effects. Again, abnormally high temperatures have stronger impacts on production than precipitation. Rice, for example, tend to be more affected by abnormal hot temperatures and the effect lasts at least four months after the shock when the latter happen during the growing period. Maize appears also to be significantly harmed by warmer temperatures during the growing stage, while the responses



Notes: The panels show the crop and season specific impulse responses of monthly agricultural production to a 1 SD increase in the weather variable. The weather variable is temperature anomaly for the first row and precipitation anomaly for the second row. Horizon 0 is the month of the shock. The bands formed by the grey area and the green dashed lines represent the 95% confidence intervals with standard errors clustered at the region-level, for the growing season regime and the harvesting season regime, respectively.

Figure 7: Agricultural production response to a weather shock contrasting for growing vs. harvesting season

during the harvesting season and following rises in precipitation are weaker, in line with the results of [Lobell et al. \(2013\)](#). In cumulative terms, the response of rice and maize implies a cumulative loss of about 30 to 40 percentage points, which highlights the particular vulnerability of these two crops during their growing stage.

6 From Regional to Aggregate Fluctuations

Are regional weather shocks important enough to spread to the rest of the economy? Weather shocks tend to be serially correlated across regions because these regions share common atmospheric, soil, or topographic patterns. Therefore, a weather shock may entail macroeconomic fluctuations if the number of regions affected by the same weather pattern is large enough. On policy grounds, the quantitative assessment of weather shocks on macroeconomic fluctuations is particularly important for the design of mitigation policies. For example, if a region experiences a negative shock, monetary and fiscal policies can be used

to support economic activity and cushion the impact of the shock.

The literature typically provides a synthetic measure of the weather based on average measures of county-level weather shocks and analyze its interaction with macroeconomic time series (see, *e.g.*, Natoli, 2022; Gallic and Vermandel, 2020). In contrast, we propose to measure the macroeconomic effects of the weather through the weather-implied losses measured by our baseline local projections in Equation 7. More specifically, we compute an aggregate measure W_t as follows:

$$W_t = \sum_{c=1}^R \omega_{c,t} \left[\sum_{h=0}^H (\beta_{c,T}^h T_{i,c,t-h} + \beta_{c,P}^h P_{i,c,t-h}) \right], \quad (15)$$

where $\omega_{c,t}$ is a weight measuring the relative size of crop c in the total value added among all crops at time t , while $\beta_{c,T}^h$ and $\beta_{c,P}^h$ are the marginal effects estimated previously in the baseline LPs. Intuitively, W_t measures the percentage loss in agricultural value added from weather shocks.

A vector auto-regressive (VAR) model is a straightforward way to quantitatively assess dynamic interactions across time series. A typical VAR model with p lags reads:

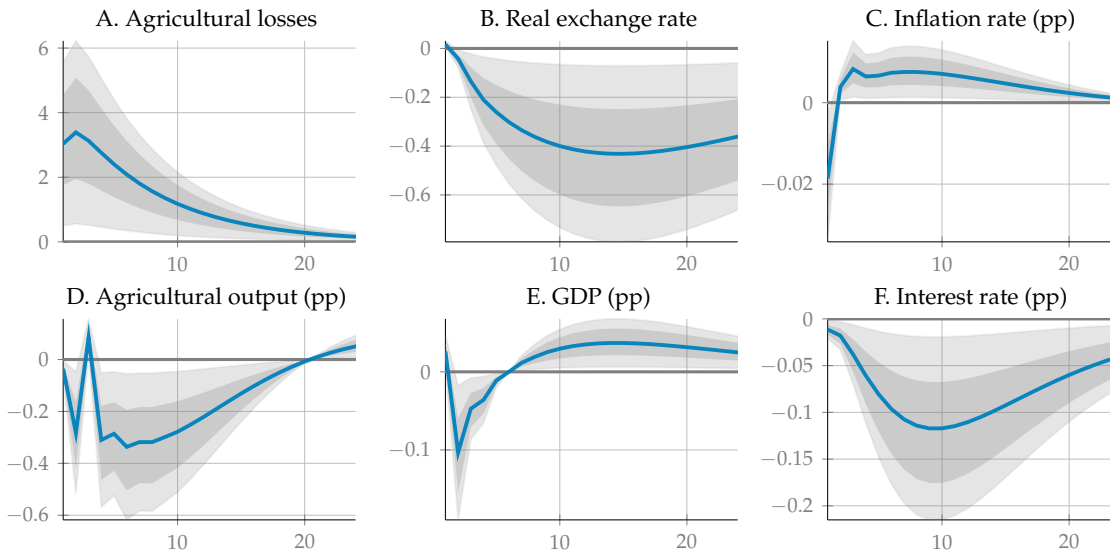
$$Y_t = \phi_0 + \sum_{i=1}^p \phi_i Y_{t-i} + \varepsilon_t, \quad (16)$$

where Y_t is a $N \times 1$ vector of endogenous variables, ε_t denotes the error term, normally distributed with zero mean and variance Σ_ε , ϕ_0 is a $N \times 1$ vector stacking constant terms and ϕ_i are $N \times N$ matrices gathering dynamic interactions across endogenous variables. The optimal number of lag p is often determined by the Akaike information criterion.

The vector of endogenous variables comprises six endogenous variables: $Y_t = [W_t \ \pi_t \ RER_t \ y_t^A \ y_t \ r_t]$. In this expression, W_t denotes the aggregate measure of weather-driven agricultural losses, π_t is the percentage change of the Consumer Price Index (CPI), RER_t denotes the Real Exchange Rate (RER), y_t^A our measure of agricultural output, y_t the GDP, and r_t the interbank rate in Peru.²² Variables exhibiting a trend (namely agricultural output and GDP) are expressed in percentage deviation from the Hodrick-Prescott trend, while seasonal components are removed with the X13 method of the Census Bureau. Our sample covers the period 2003M1–2015M12.

²²Data are all taken from Peru Central Bank, the CPI token is *PN01270PM*, the RER *PN01259PM*, GDP *PN01773AM*, interest rate *PN07819NM*.

With the Cholesky factorization of the reduced form VAR covariance matrix, the order of the variable matters. To impose full exogeneity in the weather process, we follow Gallic and Vermandel (2020) by ordering first the weather-driven agricultural-losses equation in the VAR, and muting cross-interactions with other variables. Following the ordering scheme of Stock and Watson (2001), we next order prices variables, followed by quantities and terminate with interest rates. The idea is mainly that prices variables are relatively more driven by exogenous factors (*e.g.*, oil prices shocks), while the interest rate is the most endogenous variable that reacts in contemporaneous changes in prices and quantities.



Notes: The plain blue line is the Impulse Response Function. The gray band represents 95% and 68% error bands obtained from 10,000 Monte-Carlo simulations. The response horizon is in months.

Figure 8: VAR(2) system response to one standard deviation orthogonal shock to the weather aggregate cost equation

The number of lags selected by the AIC criterion is 2. Figure 8 reports the system response to a one standard deviation increase in agricultural output from weather shocks. A rise by 4% of losses in the agricultural sector from weather shocks entails a persistent reduction of 0.5% in the real exchange rate, mainly because exports in the agricultural sector are lower. The scarcity of agricultural goods, combined with an increased prices of imports, directly affect the consumers price index and creates a relatively small surge in inflation. The inflationary effect of weather shock contrasts with the findings of Natoli (2022) and Faccia et al. (2021), who both find a lower than usual inflation following a temperature shock.

In terms of quantities, this shock in the agricultural loss equation from weather shocks generates a reduction in agricultural output by 0.4% below its trend, while GDP is 0.1%

below its trend, but is followed by a modest expansion. This delayed expansion can be rationalized by the reduction in the real exchange rate that typically boosts exports. Finally, the central bank faces a trade-off between inflation and quantity stabilization, as both are going in opposite directions. The VAR model suggests that the Peruvian central bank favor output stabilization when weather shocks occur by easing monetary conditions.

Our quantitative assessment of the macroeconomic cost of weather shocks are fairly in line with the literature. The response of output and the interest rate are very close to the findings of [Natoli \(2022\)](#) for the US economy for temperatures anomalies. Our results are also in line with the VAR model of [Gallic and Vermandel \(2020\)](#) for New Zealand, as they also obtain a GDP decrease by 0.1%, 1% for the agricultural output and a decline by 0.4% of the real exchange rate, following a drought shock.

7 Discussion and conclusion

Many efforts in the literature have been devoted to quantitatively measure how the weather is an important driver of the supply of agricultural goods. This paper contributes to this effort by analyzing the propagation mechanism of a weather shock on agricultural production at a monthly frequency, for various crops, in heterogeneous geographical and seasonal patterns. We find that the growing process of crop generates a time lag between the realization and the economic loss of the weather. An increase in both temperatures and precipitation leads to decline in production, for up to four consecutive months for any crop in our sample. Responses appear to vary both in magnitude and duration depending on the crop, with negative effects primarily driven by abnormally warm temperatures rather than increased precipitation. We analyze further these responses by distinguishing between the main geographical zones that composes Peru: the Coast, the Highlands and the Forest. This decomposition allows us to observe disparities in the climate and points out crop-specific responses when the shocks hit a zone rather than another. Responses turn out to be quite different, with negative impacts of warmer temperatures on rice production in the Forest region compared to a positive one in the two other regions for example. As highlighted by the agronomic literature ([Hatfield and Prueger, 2015](#)), responses of crops yields to weather shocks highly depend on the stage of development of the plant. We consider this point in a third section and find indeed that for each type of crop, production is harmed when the weather shock happens during the growing period, but hardly at all during the harvesting phase. This result highlights the importance of the timing of the shock, confirming that

weather anomalies arising at early growing stage have more prejudicial repercussions. Finally, we build on local projections to create a novel index of weather-driven losses. We find that a representative shock in weather-driven loss shock cause a 0.4% loss in agricultural output, leading to a 0.1% reduction in GDP.

Our findings have substantial policy implications. First, using our estimates can be informative for policymakers to anticipate the future scarcity of agricultural products arising few months after the realization of the weather shock. A government observing an adverse weather shock can import agricultural products from other regions and countries to mitigate its detrimental effects, before the economic consequences of the weather materialize at the harvesting stage. By dampening local fluctuations, such policies could be beneficial at a macroeconomic level, in particular for central banks to target price stability. Our findings are also useful in the perspective of global warming, by identifying crops and regions that are the most weather-sensitive. Adaptation to climate change implies diversifying agricultural supply toward crops that more resistant to droughts, or to flooded and waterlogged conditions.

This article also opens the avenue for future research on weather shocks at higher frequencies. First, the analysis could be extended to investigate price responses to weather variations rather than quantities. The literature (Faccia et al., 2021; Natoli, 2022), based on macroeconomic quarterly data finds that aggregate prices decline following temperature shocks. Based on more granular data exploiting the cross-section of regions and crops, the analysis could investigate whether this disinflation nature of the weather holds at a regional level. Second, future research could be devoted to understand how El Niño events are anticipated by farmers. Local market prices and quantities could react differently when the weather shock is a surprise or an anticipated news. Finally, the analysis could also be extended to analyze how local weather shocks can spread to other regions through trade interlinkages. With that respect, accommodating the international trade gravity model seems a promising avenue for future research.

8 Bibliography

Acevedo, S., Mrkaic, M., Novta, N., Pugacheva, E. and Topalova, P. (2020). The effects of weather shocks on economic activity: what are the channels of impact? *Journal of Macroeconomics* 65: 103207. 6

Aragón, F. M., Oteiza, F. and Rud, J. P. (2021). Climate change and agriculture: Subsistence

- farmers' response to extreme heat. American Economic Journal: Economic Policy 13: 1–35, doi:10.1257/pol.20190316. 2, 13
- Asseng, S., Ewert, F., Martre, P., Rötter, R. P., Lobell, D. B., Cammarano, D., Kimball, B. A., Ottman, M. J., Wall, G. W., White, J. W., Reynolds, M. P., Alderman, P. D., Prasad, P. V. V., Aggarwal, P. K., Anothai, J., Basso, B., Biernath, C., Challinor, A. J., Sanctis, G. D., Doltra, J., Fereres, E., Garcia-Vila, M., Gayler, S., Hoogenboom, G., Hunt, L. A., Izaurralde, R. C., Jabloun, M., Jones, C. D., Kersebaum, K. C., Koehler, A.-K., Müller, C., Kumar, S. N., Nendel, C., O'Leary, G., Olesen, J. E., Palosuo, T., Priesack, E., Rezaei, E. E., Ruane, A. C., Semenov, M. A., Shcherbak, I., Stöckle, C., Stratonovitch, P., Streck, T., Supit, I., Tao, F., Thorburn, P. J., Waha, K., Wang, E., Wallach, D., Wolf, J., Zhao, Z. and Zhu, Y. (2014). Rising temperatures reduce global wheat production. Nature Climate Change 5: 143–147, doi:10.1038/nclimate2470. 4
- Auerbach, A. and Gorodnichenko, Y. (2011). Fiscal Multipliers in Recession and Expansion. Tech. rep., doi:10.3386/w17447. 23, 24, 25
- Barrios, S., Bertinelli, L. and Strobl, E. (2010). Trends in rainfall and economic growth in africa: A neglected cause of the african growth tragedy. Review of Economics and Statistics 92: 350–366, doi:10.1162/rest.2010.11212. 8
- Blanc, E. and Schlenker, W. (2017). The use of panel models in assessments of climate impacts on agriculture. Review of Environmental Economics and Policy 11: 258–279, doi:10.1093/reep/rex016. 5
- Buchhorn, M., Smets, B., Bertels, L., De Roo, B., Lesiv, M., Tsendbazar, N.-E., Herold, M. and Fritz, S. (2020). Copernicus global land service: Land cover 100m: collection 3: epoch 2019: Globe. Version V3. 0.1)[Data set] doi:10.5281/zenodo.3939050. i, ii
- Burke, M. and Emerick, K. (2016). Adaptation to climate change: Evidence from us agriculture. American Economic Journal: Economic Policy 8: 106–40, doi:10.1257/pol.20130025. 2, 4
- Colacito, R., Hoffmann, B. and Phan, T. (2019). Temperature and growth: A panel analysis of the united states. Journal of Money, Credit and Banking 51: 313–368. 2, 4, 10
- Crost, B., Duquennois, C., Felter, J. H. and Rees, D. I. (2018). Climate change, agricultural production and civil conflict: Evidence from the philippines. Journal of Environmental Economics and Management 88: 379–395, doi:10.1016/j.jeem.2018.01.005. 19

- D'Agostino, A. L. and Schlenker, W. (2016). Recent weather fluctuations and agricultural yields: implications for climate change. Agricultural Economics 47: 159–171, doi:10.1111/agec.12315. 2, 4, 5, 9
- Dell, M., Jones, B. F. and Olken, B. A. (2012). Temperature shocks and economic growth: Evidence from the last half century. American Economic Journal: Macroeconomics 4: 66–95, doi:10.1257/mac.4.3.66. 3, 16
- Dell, M., Jones, B. F. and Olken, B. A. (2014). What do we learn from the weather? The new climate-economy literature. Journal of Economic Literature 52: 740–798, doi:10.1257/jel.52.3.740. 2
- Deschênes, O. and Greenstone, M. (2007). The economic impacts of climate change: evidence from agricultural output and random fluctuations in weather. American economic review 97: 354–385, doi:10.1257/aer.97.1.354. 2, 4
- Faccia, D., Parker, M. and Stracca, L. (2021). Feeling the heat: extreme temperatures and price stability . 4, 29, 31
- Funk, C., Peterson, P., Landsfeld, M., Pedreros, D., Verdin, J., Shukla, S., Husak, G., Rowland, J., Harrison, L., Hoell, A. et al. (2015). CHIRPS: Rainfall estimates from rain gauge and satellite observations. doi:10.15780/G2RP4Q. 9
- Gallic, E. and Vermandel, G. (2020). Weather shocks. European Economic Review 124: 103409, doi:10.1016/j.eurocorev.2020.103409. 28, 29, 30
- Hatfield, J. L. and Prueger, J. H. (2015). Temperature extremes: Effect on plant growth and development. Weather and climate extremes 10: 4–10, doi:10.1016/j.wace.2015.08.001. 26, 30
- Huerta, A., Aybar, C. and Lavado-Casimiro, W. (2018). PISCO temperatura v.1.1. Tech. rep., SENAMHI - DHI, Lima-Perú. 9
- Iizumi, T. and Ramankutty, N. (2015). How do weather and climate influence cropping area and intensity? Global Food Security 4: 46–50, doi:10.1016/j.gfs.2014.11.003. 3
- Jagnani, M., Barrett, C. B., Liu, Y. and You, L. (2020). Within-season producer response to warmer temperatures: Defensive investments by kenyan farmers. The Economic Journal 131: 392–419, doi:10.1093/ej/ueaa063. 2, 5
- Jordà, Ò. (2005). Estimation and inference of impulse responses by local projections. American economic review 95: 161–182, doi:10.1257/0002828053828518. 3, 17

- Kolstad, C. D. and Moore, F. C. (2020). Estimating the economic impacts of climate change using weather observations. Review of Environmental Economics and Policy 14: 1–24, doi:10.1093/reep/rez024. 4, 5
- Lesk, C., Rowhani, P. and Ramankutty, N. (2016). Influence of extreme weather disasters on global crop production. Nature 529: 84–87, doi:10.1038/nature16467. 3
- Letta, M., Montalbano, P. and Pierre, G. (2022). Weather shocks, traders’ expectations, and food prices. American Journal of Agricultural Economics 104: 1100–1119, doi:10.1111/ajae.12258. 23
- Lobell, D. B., Hammer, G. L., McLean, G., Messina, C., Roberts, M. J. and Schlenker, W. (2013). The critical role of extreme heat for maize production in the united states. Nature climate change 3: 497–501. 27
- Masseti, E., Mendelsohn, R. and Chonabayashi, S. (2016). How well do degree days over the growing season capture the effect of climate on farmland values? Energy Economics 60: 144–150, doi:10.1016/j.eneco.2016.09.004. 23
- Mendelsohn, R. (2009). The impact of climate change on agriculture in developing countries. Journal of Natural Resources Policy Research 1: 5–19, doi:10.1080/19390450802495882. 2
- Mendelsohn, R., Nordhaus, W. D. and Shaw, D. (1994). The impact of global warming on agriculture: a ricardian analysis. The American economic review : 753–771. 4
- Natoli, F. (2022). Temperature surprise shocks. Tech. rep., doi:10.2139/ssrn.4160944. 6, 28, 29, 30, 31
- Ortiz-Bobea, A., Ault, T. R., Carrillo, C. M., Chambers, R. G. and Lobell, D. B. (2021). Anthropogenic climate change has slowed global agricultural productivity growth. Nature Climate Change 11: 306–312, doi:10.1038/s41558-021-01000-1. 4
- Ortiz-Bobea, A. and Just, R. E. (2012). Modeling the structure of adaptation in climate change impact assessment. American Journal of Agricultural Economics 95: 244–251, doi:10.1093/ajae/aas035. 5
- Ortiz-Bobea, A., Wang, H., Carrillo, C. M. and Ault, T. R. (2019). Unpacking the climatic drivers of US agricultural yields. Environmental Research Letters 14: 064003, doi:10.1088/1748-9326/ab1e75. 5
- Parry, M., Canziani, O., Palutikof, J., Linden, P. van der and Hanson, C. (2007). Fourth assessment report: Climate change 2007: The ar4 synthesis report. Geneva: IPCC. URL <http://www.ipcc.ch/ipccreports/ar4-wg1.htm> . 3, 9

- Powell, J. and Reinhard, S. (2016). Measuring the effects of extreme weather events on yields. Weather and Climate Extremes 12: 69–79, doi:[10.1016/j.wace.2016.02.003](https://doi.org/10.1016/j.wace.2016.02.003). 4, 5
- Rosenzweig, C., Elliott, J., Deryng, D., Ruane, A. C., Müller, C., Arneth, A., Boote, K. J., Folberth, C., Glotter, M., Khabarov, N., Neumann, K., Piontek, F., Pugh, T. A. M., Schmid, E., Stehfest, E., Yang, H. and Jones, J. W. (2013). Assessing agricultural risks of climate change in the 21st century in a global gridded crop model intercomparison. Proceedings of the National Academy of Sciences 111: 3268–3273, doi:[10.1073/pnas.1222463110](https://doi.org/10.1073/pnas.1222463110). 4
- Schlenker, W. and Roberts, M. J. (2009). Nonlinear temperature effects indicate severe damages to us crop yields under climate change. Proceedings of the National Academy of sciences 106: 15594–15598, doi:[10.1073/pnas.0906865106](https://doi.org/10.1073/pnas.0906865106). 4, 5
- Schmitt, J., Offermann, F., Söder, M., Frühauf, C. and Finger, R. (2022). Extreme weather events cause significant crop yield losses at the farm level in german agriculture. Food Policy 112: 102359, doi:[10.1016/j.foodpol.2022.102359](https://doi.org/10.1016/j.foodpol.2022.102359). 4, 5
- Skees, J. R., Hartell, J. and Murphy, A. G. (2007). Using index-based risk transfer products to facilitate micro lending in peru and vietnam. American Journal of Agricultural Economics 89: 1255–1261, doi:[10.1111/j.1467-8276.2007.01093.x](https://doi.org/10.1111/j.1467-8276.2007.01093.x). 19
- Stock, J. H. and Watson, M. W. (2001). Vector autoregressions. Journal of Economic Perspectives 15: 101–115, doi:[10.1257/jep.15.4.101](https://doi.org/10.1257/jep.15.4.101). 29
- Welch, J. R., Vincent, J. R., Auffhammer, M., Moya, P. F., Dobermann, A. and Dawe, D. (2010). Rice yields in tropical/subtropical asia exhibit large but opposing sensitivities to minimum and maximum temperatures. Proceedings of the National Academy of Sciences 107: 14562–14567, doi:[10.1073/pnas.1001222107](https://doi.org/10.1073/pnas.1001222107). 4, 5, 23

INTERNET APPENDIX

(not for publication)

A Data

[Table A.1](#) reports the total harvested area of Peru’s main crops and their share of total annual production between 2001 and 2015. The surface area figures on which the article is based, i.e., those from the files of the Ministry of Agriculture of Peru (MINAGRI), are very close to those reported by the FAO. Those pertaining to the relative share of each crop are higher in the Ministry data. The crops included in the analyses carried out in the article represent almost two-thirds of production.

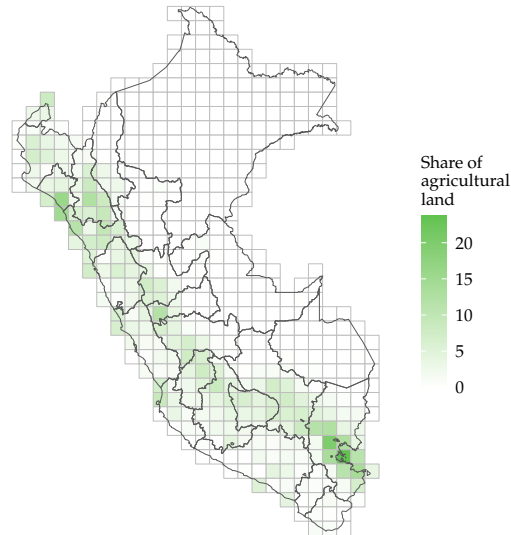
Table A.1: Main agricultural cultures in Peru

Product	FAO data		MINAGRI data	
	Total surface	Share	Total surface	Share (%)
Maize				
Starchy corn	7,349,640	16.4	4,227,147	14.7
Rice, paddy	5,359,251	12.0	2,948,963	10.3
Coffee, green	4,999,410	11.1	5,320,330	18.5
Potatoes	4,213,436	9.4	-	-
Barley	4,999,410	11.1	4,151,734	14.5
Plantains and others	2,253,611	5.0	2,233,429	7.8
Wheat	2,227,709	5.0	-	-
Cassava	2,158,122	4.8	2,102,246	7.3
Sugar cane	1,425,493	3.2	1,418,054	4.9
Beans, dry	1,112,131	2.5	1,032,231	3.6
	1,104,473	2.5	686,788	2.4

Notes: Products shown in bold are those studied in this article. Total surfaces correspond to the sum of national harvested surfaces, from 2001 to 2015, in hectares. Maize corresponds to Dent corn in the MINAGRI data. No distinction is made between Dent corn and Starchy corn in FAO data.

Source: FAO and MINAGRI. Author’s estimate.

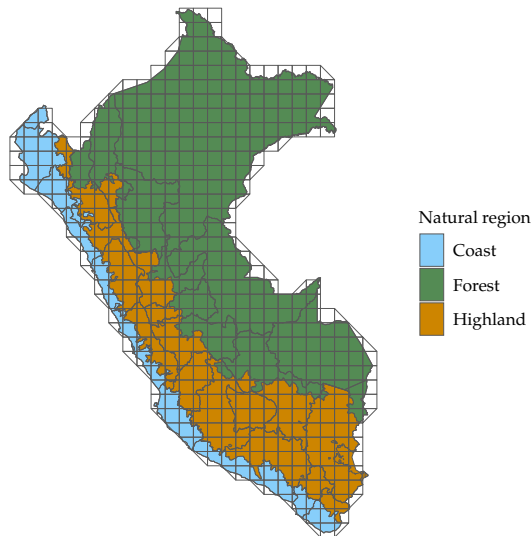
The map in [Figure 2](#) shows the percentage of agricultural land for each cell corresponding to the weather data grid. These percentages are calculated from the Land Cover map data ([Buchhorn et al., 2020](#)). It can be noted that the agricultural land is mainly located on the coastal regions and in the highlands, as shown in [Figure A.1](#) and [Figure A.2](#).



Notes: 2015 data, 100m resolution.

Source: Author's estimate using data from [Buchhorn et al. \(2020\)](#).

Figure A.1: Agricultural area for each grid cell



Source: Geo GPS Peru.

Figure A.2: Natural regions in Peru